Solar-Terrestrial Physics. 2022. Vol. 8. Iss. 3. P. 38–45. DOI: 10.12737/stp-83202206. © 2022
Belyuchenko K.V., Klimenko M.V., Klimenko V.V., Ratovsky K.G. Published by INFRA-M Academic Publishing House

UDC 551.510.535
DOI: 10.12737/stp-83202206

Received April 20, 2022
Accepted July 03, 2022

CONNECTION OF TOTAL ELECTRON CONTENT DISTURBANCES WITH *AE* INDEX OF GEOMAGNETIC ACTIVITY DURING GEOMAGNETIC STORM IN MARCH 2015

K.V. Belyuchenko
Immanuel Kant Baltic Federal University, Kaliningrad, Russia, kdei@list.ru

M.V. Klimenko
West Department of Pushkov Institute of Terrestrial Magnetism, Ionosphere and Radio Wave Propagation RAS, Kaliningrad, Russia, maksim.klimenko@mail.ru

V.V. Klimenko
West Department of Pushkov Institute of Terrestrial Magnetism, Ionosphere and Radio Wave Propagation RAS, Kaliningrad, Russia, vvk_48@mail.ru

K.G. Ratovsky
Institute of Solar-Terrestrial Physics SB RAS, Irkutsk, Russia, ratovsky@iszf.irk.ru

Abstract. Ionospheric response to the March 17, 2015 geomagnetic storm has been investigated using simulations of the Global Self-consistent Model of the Thermosphere, Ionosphere, Protonosphere (GSM TIP) [Dmitriev et al., 2017; Klimenko et al., 2018]. GSM TIP demonstrates results that do not contradict experimental data. This paper deals with GSM TIP simulated disturbances in the Total Electron Content (*TEC*) at different longitudes and zonal averages on March 17–23, 2015. At all longitudes, we can observe the existence of a band of *TEC* positive disturbances, located over the geomagnetic equator, and the formation of an after-storm ionospheric effect that appeared as positive *TEC* disturbances at midlatitude 3–5 days after the geomagnetic storm main phase. We have analyzed the dependence of disturbances of the thermosphere-ionosphere system (total electron content, $n(N_2)$, $n(O)$, zonal electric field, meridional component of the thermospheric wind at a height of 300 km, and electron temperature at a height of 1000 km), calculated by GSM TIP from variations in the geomagnetic activity index *AE*. The analysis is based on Pearson's correlation coefficients, presented as maps of the dependence of the correlation coefficient on UT and latitude for selected longitudes and for zonal averaged values. The results suggest that at high latitudes of the Northern and Southern hemispheres the correlation coefficient of *TEC* disturbances and *AE* variations is close to 1 at all longitudes in the period from 12 UT to 23 UT. From 9 UT to 12 UT, the minimum value of the correlation coefficient is observed at all latitudes and longitudes. The time intervals of the correlation values are associated with the features of a particular geomagnetic storm, for which, for example, the interval from 12 UT to 23 UT on March 17, 2015 corresponds to the geomagnetic storm main phase. We discuss possible mechanisms for the formation of such a relationship between simulated *TEC* disturbances and the *AE* index.

Keywords: geomagnetic storm, ionospheric disturbances, GSM TIP.

INTRODUCTION

Geomagnetic disturbances (magnetic storms and substorms) are one of the most important objects of research in solar-terrestrial physics and the most significant space weather events. Magnetospheric (geomagnetic) disturbance intensity is estimated by the geomagnetic indices $K_p(A_p)$, *Dst*, and *AE*. The high-latitude *AE* index characterizes the auroral current intensity and is an indicator of substorm activity [Davis, Sugiura, 1966]. The low-latitude *Dst* index is used to estimate the ring current intensity during magnetic storms and is a measure of geoeffectiveness of interplanetary disturbances [Sugiura, 1964; Burton et al., 1975]. Gonzalez et al. [1994, 1999] have defined geomagnetic storms in terms of *Dst* behavior and have classified magnetic storms by their effectiveness.

Magnetospheric processes through precipitation of energetic particles, Joule heating, magnetosphere-ionosphere currents, and magnetospheric convection electric fields have a significant impact on Earth's ionosphere [Buonsanto, 1999; Mendillo, 2006; Prölss, 1995, 2013]. When studying the ionospheric response to geomagnetic storms, disturbances observed during the storm main phase are usually considered since it is precisely during this period that ionospheric disturbances are most intense. It is widely accepted that at high and middle latitudes a negative ionospheric storm is caused by redistribution of temperature, composition, and density of the thermosphere during magnetic storms [Buonsanto, 1999; Mayr, Volland, 1973]. The ionospheric effect of a strong geomagnetic storm may last for several days [Shpynev et al., 2018]. The question about the formation of ionospheric disturbances during the geomagnetic storm recovery phase has recently been actively discussed [Balan et al., 2013; Suvorova et al., 2013]. Studies into the ionospheric response to geomagnetic storms through statistical analysis, carried out in [Ratovsky et al., 2018; Ratovsky et al., 2020], have shown that there are ionospheric after-storm effects, interpreted based on calculations by the upper atmosphere model [Klimenko et al., 2017; Ratovsky et al., 2018]. Statistical studies have also revealed that iono-

spheric disturbances can vary widely from event to event, even though the general patterns of behavior of ionospheric parameters during geomagnetic disturbances are known.

Deminov et al. [2017] have proposed a method of identifying the contribution of geomagnetic activity to the median of the F2-layer critical frequency f_oF2 at midlatitudes. The method was used to derive f_oF2 dependences on A_p, averaged over a month, thereby making it possible to predict median f_oF2 with respect to geomagnetic activity. Deminov et al. [2021] have demonstrated that their proposed equation for the relationship between the ionospheric parameter and the solar activity index describes 95–98 % of variations in the ionospheric parameter, whereas the remainder depending on geomagnetic activity indices (derivatives of A_p) is described by linear regression. The possible dependence of the ionospheric index on A_p is due to the fact that the f_oF2 median depends not only on solar, but also on geomagnetic activity [Deminov et al., 2017]. Yagodkina et al. [2021] have used data from a mid-latitude ionospheric station (Moscow) to study the dependence of f_oF2 and the F2-layer maximum height, h_mF2, on the level of geomagnetic activity during an isolated magnetic storm on June 22–23, 2015. The most sensitive parameter responding to changes in external conditions was shown to be h_mF2. During the pre-storm period, with increasing geomagnetic activity the critical frequency decreases and the F2-layer height increases. During the storm main phase, only h_mF2 appears to be sensitive to geomagnetic activity variations. During the storm recovery phase, a decrease in geomagnetic activity is accompanied by an increase in f_oF2 and h_mF2.

A significant contribution to understanding the processes of formation of ionospheric variations associated with geomagnetic activity has been made by theoretical studies using various numerical models of the ionosphere [Pirog et al., 2006; Balan et al., 2009; Huba et al., 2017], as well as more complex models of Earth's upper atmosphere [Namgaladze et al., 2000; Fuller-Rowell et al., 2007; Lu et al., 2008; Pawlowski et al., 2008]. An insight into ionospheric variability during geomagnetic disturbances has been provided by studies based on the results of calculations made using the Global Self-consistent Model of the Thermosphere, Ionosphere, Protonosphere (GSM TIP) [Klimenko et al., 2011; Dmitriev et al., 2017]. GSM TIP accounted for geomagnetic disturbances using a model of auroral electron precipitation [Vorobjev, Yagodkina, 2008], as well as the empirical dependence of the cross polar cap potential $\Delta\Phi$ and latitudes of field-aligned currents on geomagnetic activity [Sojka et al., 1994; Feshchenko, Maltsev, 2003]. As a measure of geomagnetic activity these models utilized the *AE* and *AL* indices with 1 min time resolution, i.e. these indices are driving parameters of GSM TIP. The purpose of this work is to study the relationship between disturbances of the parameters of the thermosphere—ionosphere system, obtained from GSM TIP calculations, and variations in the geomagnetic activity indices (driving parameters of the model) during the March 17–23, 2015 geomagnetic storm.

DESCRIPTION OF THE EVENT UNDER STUDY AND THE SURVEY METHOD

In this paper, we examine ionospheric effects of the geomagnetic storm that occurred in March 2015 (St. Patrick's Storm), the most powerful geomagnetic storm (by *Dst*) in solar cycle 24. Many scientific papers have been devoted to this storm, and in 2017 a special issue of Journal of Geophysical Research was published on various aspects of the research into the response of near-Earth space to the March 2013 and 2015 geomagnetic storms (a brief overview on these studies is given in [Zhang et al., 2017]). During one of these storms in 2015, a mid-latitude aurora was detected in Eastern Siberia, which was not typical for this region [Mikhalev et al., 2018]; and two stable red arcs were observed which were spaced in latitude and differed in the heating processes occurring in them [Zolotukhina et al., 2021]. Figure 1 illustrates variations in *Dst*, *AE*, and *AL* on March 16–23, 2015. As inferred from the behavior of *Dst*, the phase of the sudden storm commencement took place on March 17 at ~06 UT, and the geomagnetic storm main phase lasted from 09 to 24 UT. Minimum *Dst*=–223 nT was recorded at ~23 UT. Maximum (in modulus) *AE* and *AL* were observed at ~14 UT and ranged up to 1200–1500 nT. The geomagnetic storm recovery phase was fairly long and had a general trend of decreasing *AE* and *AL* in the period through to March 22.

Using GSM TIP, for March 17–23, 2015 we have obtained spatial and temporal dependences of disturbances (relative to March 16, 2015 background values) of *TEC*, n(N2), n(O), zonal electric field E_{zon}, meridional wind velocity V_{tet} for a height of 300 km, and electron temperature T_e for a height of 1000 km.

In this paper, to find the possible relationship between parameters of the thermosphere—ionosphere system and *AE*, we have carried out a correlation analysis, applying the Pearson formula, which assumes that there is a linear relationship between the two values considered.

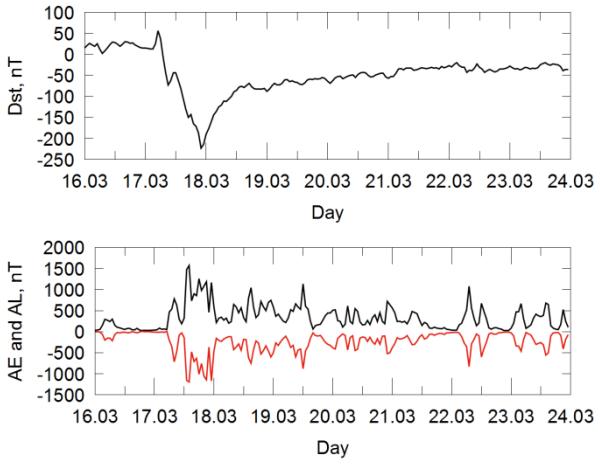

Figure 1. Variations in the geomagnetic activity indices *Dst* (top), *AE* and *AL* (bottom, black and red lines respectively) on March 16–23, 2015

$$R_{x,\,AE}(\mathrm{UT},\theta) = \frac{\sum_{i=1}^{n}\left(x_i(\mathrm{UT},\theta)-\overline{x(\mathrm{UT},\theta)}\right)\left(AE_i(\mathrm{UT})-\overline{AE(UT)}\right)}{\sqrt{\sum_{i=1}^{n}\left(x_i(\mathrm{UT},\theta)-x(\mathrm{UT},\theta)\right)^2\sum_{i=1}^{n}\left(AE_i(\mathrm{UT})-\overline{AE(UT)}\right)^2}},$$

where $\left(\overline{AE(\mathrm{UT})}\right)=\frac{1}{n}\sum_{i=1}^{n}AE_i(\mathrm{UT})$ is average AE for n days of interest for a fixed moment of UT; $n=7$ is the number of days used to calculate the correlation coefficient; i is the day number (March 17 $i=1$, March 18 $i=2$, …, March 23 $i=7$); $x_i(\mathrm{UT}, \theta)$ are the parameters calculated by GSM TIP; $\overline{x(\mathrm{UT},\theta)}$ are average parameters for 7 days under study as function of UT and latitude θ. If $R=0$, the values considered are linearly independent; for $|R|=1$, they have a linear dependence. From the correlation coefficients derived, we have drawn time-latitude dependences R of disturbances of all the above mentioned parameters of the thermosphere-ionosphere system and *AE*.

DISCUSSION AND RESULTS

Figure 2 shows variations in *TEC* disturbances at three longitudes (30° E, 105° E, 90° W) corresponding to the European, East Siberian, and American sectors, and their zonal averages, obtained by averaging the parameter of interest over longitude for given UT. The choice of the longitude sectors is governed by their different remoteness from the South and North Geomagnetic Poles. GSM TIP uses the following geographic coordinates of the North and South Poles: 78.6° N, 69.5° W and 78.6° S, 110.5° E respectively. The analysis of maps of zonal average *TEC* disturbances has revealed that the most intense disturbances occurred during the storm main phase on March 17 from 09 to 24 UT at middle and high latitudes (30° N, 90° N) and (30° S, 90° S). On the second day, at the beginning of the recovery phase, maximum negative disturbances were clearly visible at all latitudes with maxima in the vicinity of both poles and at the equator. From 00 UT on March 20, positive *TEC* disturbances intensifying from day to day were also formed at all latitudes from the equator to the pole. The analysis of the *TEC* disturbances at different longitudes shows both their similarity (positive disturbances during the storm main phase; negative disturbances the next day; the occurrence of dayside positive and nightside negative effects throughout the long recovery phase of the geomagnetic storm) and differences (different latitudinal structure of *TEC* disturbances during the storm main phase, latitudinal extent and magnitude of positive and negative *TEC* disturbances during the recovery phase).

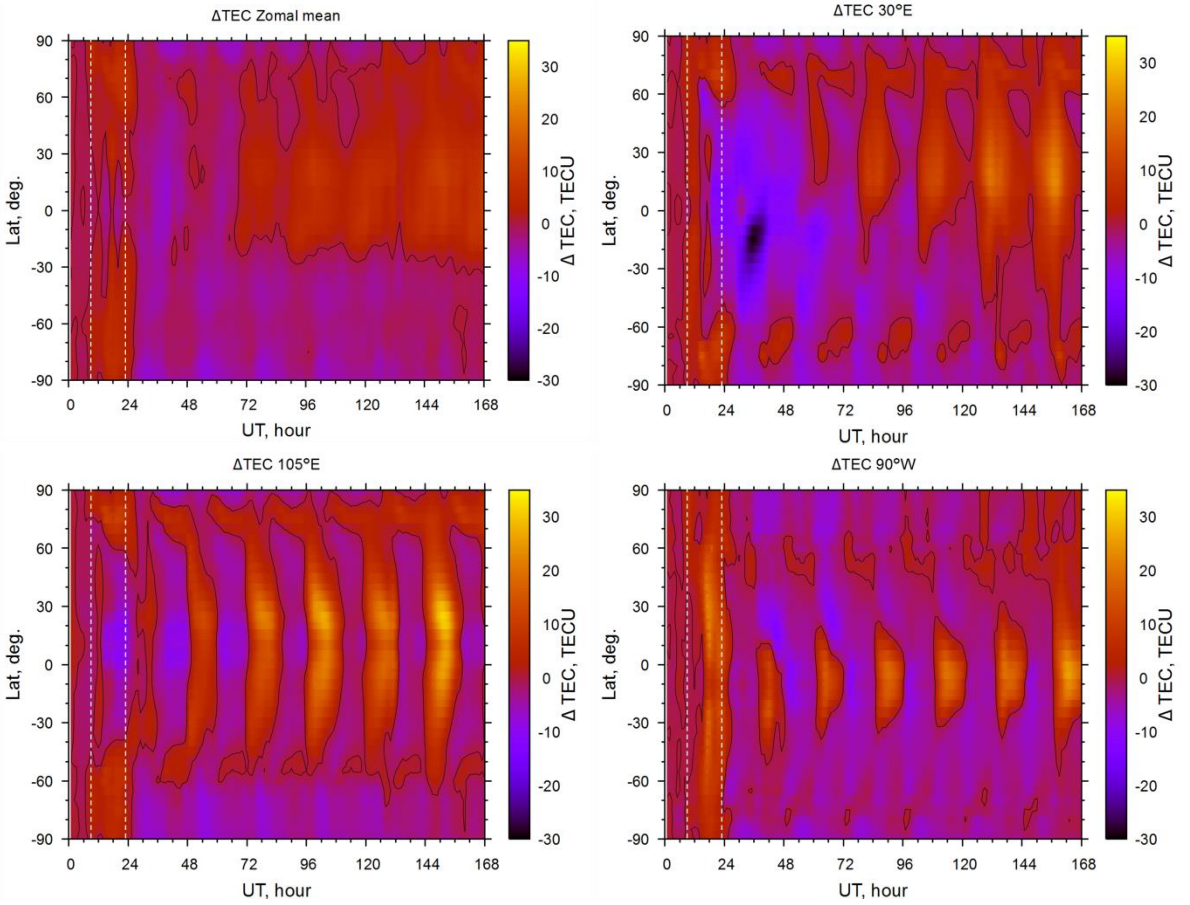

Figure 2. Latitude-time variations in *TEC* disturbances of zonal means (*a*); at longitudes of 30° E (*b*), 105° E (*c*), and 90° W (*d*) on March 17–23, 2015. The zero hour corresponds to 00 UT on March 17. Black lines are isolines of zero *TEC* disturbances; dashed lines indicate the storm main phase

It is significant that the most intense and latitudinally extensive positive *TEC* disturbances during the recovery phase are formed at longitudes of 30° E and 105° E. At 90° W, these disturbances are concentrated in the equatorial region. At 105° E and 90° W, they are symmetric about the equator; and for 30° E, an interhemispheric asymmetry is formed with a shift of positive disturbances to the Northern Hemisphere. Thus, we can conclude that the previously identified after-storm effects [Klimenko et al., 2017; Ratovsky et al., 2018; Ratovsky et al., 2020] are manifested at all longitudes, but with different degrees of intensity and latitude coverage. At the same time, the highest intensity and coverage of the after-storm effect takes place in the East Siberian sector; the lowest intensity, in the American one. The longitude dependence of the after-storm effect has been found for the first time, and the presence of after-storm effects for all UT moments in zonal mean *TEC* disturbances has been noted. An important result is also the presence of interhemispheric asymmetry of the after-storm effect that manifests itself mainly in the Northern Hemisphere.

Figure 3 presents maps of correlations between *AE*, *TEC* disturbances for longitudes of 30° E, 105° E, 90° W and zonal mean disturbances in UT—latitude coordinates. It may be noted that for all the maps in hand the correlation coefficient has quite high positive values (from 0.65 to 0.9) at high latitudes during the period from 12 to 24 UT. In this case, the correlation is higher in the Southern Hemisphere than in the Northern one. Similar high values of anticorrelation (from –0.4 to –0.8) appear in the equatorial zone in the same time interval. Anticorrelation regions are formed at all longitudes under study for all latitudes from 09 to 12 UT. From 00 to 04 UT there is a positive correlation for zonal mean *TEC* and for disturbances at the longitude of 105° E. During the same period, a negative correlation can be observed between *AE* and *TEC* disturbances for 30° E and 90° W at middle and low latitudes. Approximately from 06 to 09 UT, the picture changes to the opposite, i.e. for zonal mean *TEC* and at 105° E a negative correlation is observed at middle and low latitudes; for 30° E and 90° W, a positive correlation.

When comparing Figures 1 and 3, we can note a dependence *R* on daily variations in *AE* on the first and second days of the storm. For instance, at the beginning of the storm we can see a slight increase in *AE* from 50 to 700 nT, to which correspond low values of the correlation coefficient (~0.2) during the period from 06 to 09 UT. In this case, for 105° E and for zonal means the positive correlation during the said period is at high latitudes. This is followed by a decrease in *AE* to 150 nT (09–12 UT), to which correspond anticorrelation regions of *TEC* disturbances and *AE* (from –0.4 to –0.8). To a sharp increase in *AE* during the storm main phase corresponds the appearance of large positive correlation values at high latitudes and anticorrelation in the equatorial zone (12–24 UT). For clarity, Figure 4 gives an example of day-to-day *AE* variations and *TEC*

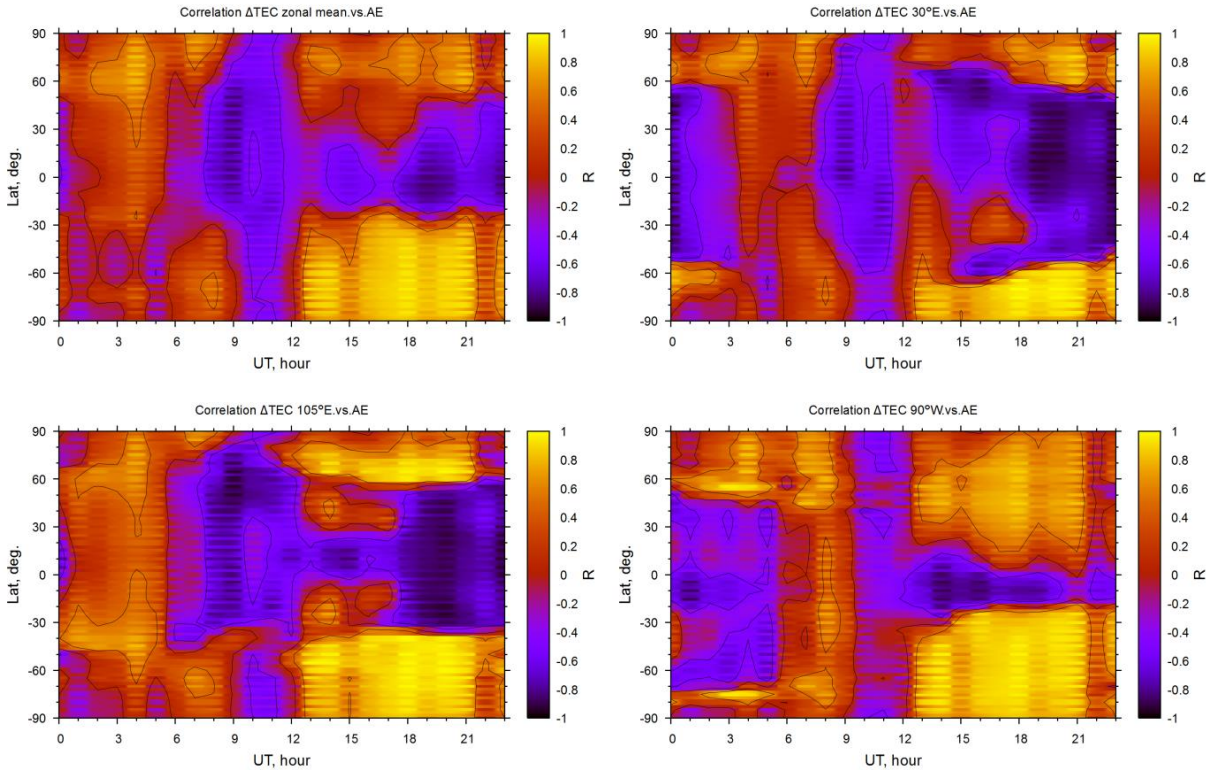

Figure 3. Maps in latitude—UT coordinates of the correlation coefficient between *AE* variations for a given hour and zonal mean *TEC* disturbances (*a*); disturbances at longitudes of 30° E (*b*), 105° E (*c*), and 90° W (*d*) for a given latitude and UT on March 17–23, 2015

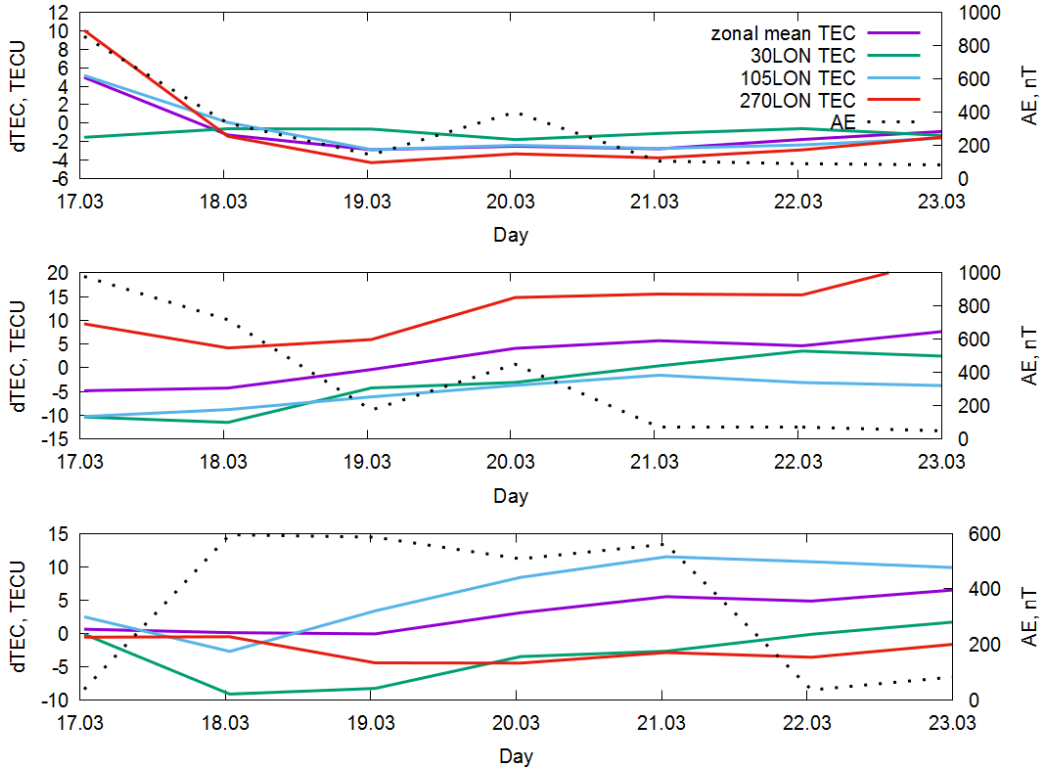

Figure 4. Day-to-day variations in the geomagnetic activity index *AE* and *TEC* disturbances at longitudes of 30° E, 105° E, 270° E and their zonal means. 1 — for 60° S at 18 UT; 2 — for the equatorial zone at 20 UT; 3 — for 30° N at 01 UT

disturbances for latitudes and time points with a correlation coefficient to 0.9 (18 UT at 60° S), anticorrelation to –0.8 (20 UT at the equator), and different correlation coefficients at different longitudes (01 UT at 30° N). We can see that maximum positive *TEC* disturbances corresponding to maximum *AE* are formed at subauroral latitudes on the first day of the storm at 18 UT (almost at all longitudes). With decreasing *AE*, *TEC* disturbances become negative, which is associated with emptying of plasma tubes during the storm main phase. Then, to the local maximum of *AE* on the fourth day correspond local maxima of *TEC* disturbances at subauroral latitudes. The opposite behavior of the *TEC* disturbances and *AE* approximately at the same time (20 UT) is observed at the equator. Minimum *TEC* disturbances (negative at almost all longitudes) are developed at the equator on the first and second days during the period of the highest *AE* values. As *AE* decreases, *TEC* disturbances become positive, which at some longitudes leads to the formation of a positive after-storm effect. At 01 UT at midlatitudes, there is practically no connection between *TEC* disturbances and *AE*.

We have also drawn maps in latitude—UT coordinates of dependences of the correlation coefficient at the 30° E longitude (as an example) between n(N2), n(O), E_{zon}, V_{tet}, T_e disturbances and *AE* variations (Figure 5). To illustrate the comparison, the *TEC* disturbance correlation map was duplicated in Figure 5. The map of correlation between n(N2) disturbances and *AE* exhibits a positive correlation before the onset of the storm during the first peak (07–09 UT) (see Figure 1), as well as a decrease in the correlation (from 0.8 to 0.2) corresponding to the *AE* decrease (at ~12 UT) on the first and second days of the storm. For the rest of the time, from 15 to 21 UT, there is a high positive correlation, which corresponds to high *AE* values at the UT moments considered on the first and second days of the storm.

An attempt to link the correlation of *TEC* disturbances and *AE* with correlations of disturbances of other parameters and *AE* has revealed the following features. There is a good correlation between Δn(N2) and *AE* for intervals of high *AE* (from ~09 UT, the storm main phase). Accordingly, at the latitudes of the positive correlation between ΔTEC and *AE*, the behavior of $R_{\Delta TEC}$ and $R_{\Delta n(N2)}$ is consistent, and it is opposite at the latitudes of the negative correlation between ΔTEC and *AE*. The correlation between Δn(O) and *AE* is quite complex. It is possible to identify a region of positive correlation (near the equator), a region of negative correlation (in the Southern Hemisphere at middle and low latitudes), and spots of positive correlation before the storm at midlatitudes. When comparing $R_{\Delta n(O)}$ and $R_{\Delta TEC}$, we can note the opposite behavior near the equator, as in the case of $R_{\Delta TEC}$ and $R_{\Delta n(N2)}$. The correlations of ΔE_{zon} and ΔV_{tet} with *AE* are quite complex. A key role is probably played by the fact that electric field and thermospheric wind disturbances are significant only on the first day of a geomagnetic storm.

Hence, the following conclusions can be drawn.

1. In some space-time domains there is physically explicable opposite behavior of the correlations between n(N2) and *TEC* disturbances. From 03 to 06 UT, positive $R_{\Delta n(N2)}$ and negative $R_{\Delta TEC}$ are formed; from 09 to 12 UT, negative $R_{\Delta n(N2)}$ and positive $R_{\Delta TEC}$; from 13 to 24 UT, regions of positive $R_{\Delta n(N2)}$ and negative $R_{\Delta TEC}$ appear at middle and low latitudes.

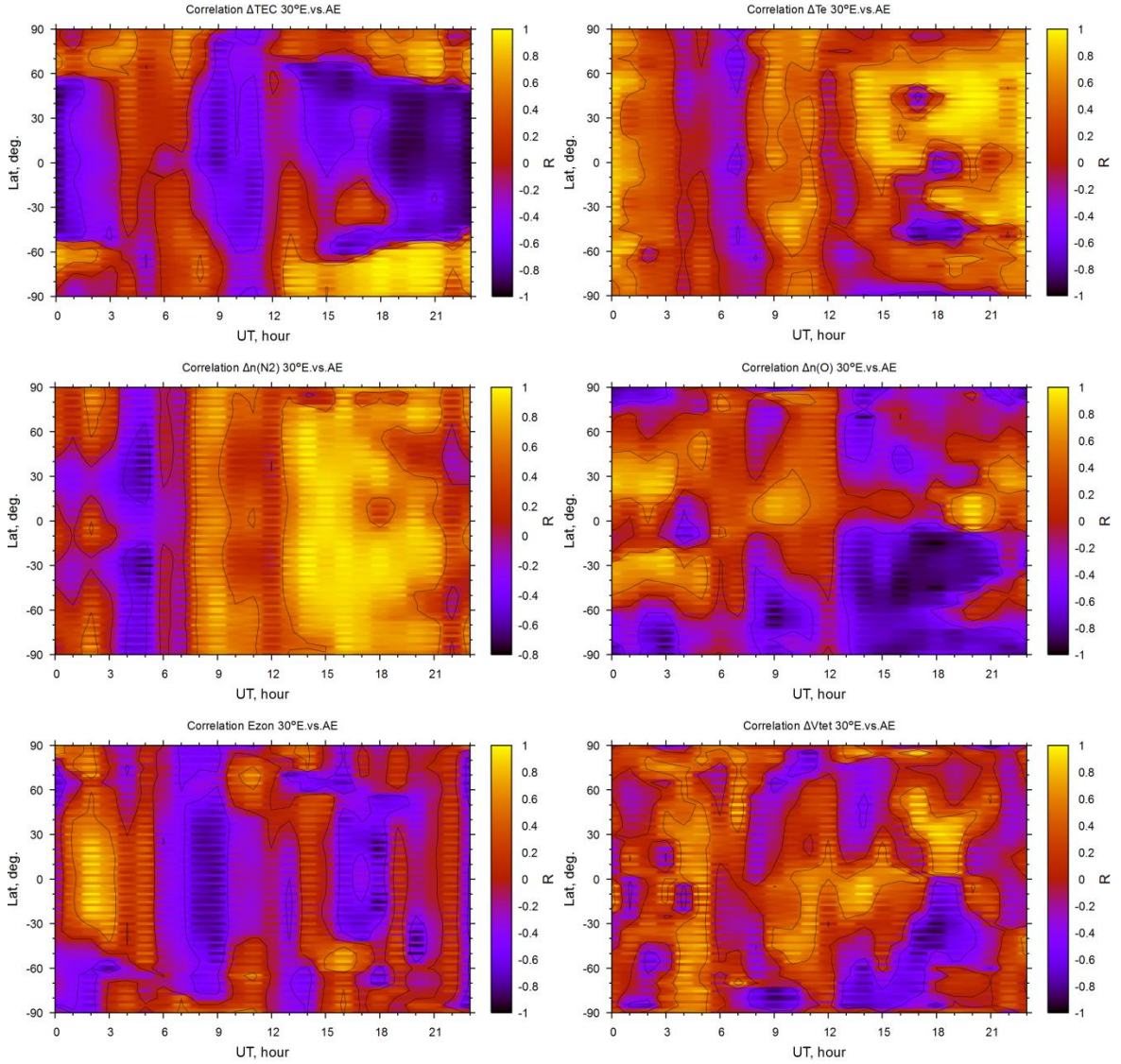

Figure 5. Maps in latitude—UT coordinates of the dependences of the correlation coefficient between *AE* and disturbances of thermosphere—ionosphere system parameters at 30° E: TEC (*a*), electron temperature (*b*), nitrogen concentration (*c*), oxygen concentration (*d*), zonal electric field (*e*), meridional thermospheric wind (*f*) on March 17–23, 2015

2. It is possible to find a similarity between $R_{\Delta n(\mathrm{O})}$ and $R_{\Delta TEC}$ at midlatitudes during daylight hours (06–19 UT).

3. There is no connection between $R_{\Delta E\mathrm{zon}}$, $R_{\Delta V\mathrm{tet}}$ and $R_{\Delta TEC}$. According to the correlation analysis results, the relationship between *TEC* and *AE* is explained by the important role of disturbances in the neutral thermosphere composition throughout March 17–23. At the same time, the role of electric field and thermospheric wind disturbances in forming *TEC* disturbances is significant only on the first day of the geomagnetic storm [Dmitriev et al., 2017; Ratovsky et al., 2020]. It is worth noting that to the ranges of high $R_{\Delta TEC}$ at high latitudes at 12–24 UT correspond high $R_{\Delta n(\mathrm{N2})}$ and negative $R_{\Delta n(\mathrm{O})}$. This suggests that the composition perturbations are not a key factor in *TEC* disturbances at high latitudes. The high-latitude positive correlation of *TEC* can be explained by the behavior of T_e having similar structures at these latitudes at 14–23 UT.

CONCLUSIONS

Analyzing the relationship of *TEC* disturbances with *AE* variations and thermosphere—ionosphere system parameters during the March 17–23, 2015 geomagnetic storm has yielded the following results.

1. Zonal mean TEC disturbances are shown to indicate the formation of the positive after-storm effect observed during daytime hours and expanding from the equator to the poles. The previously identified after-storm effects [Klimenko et al., 2017; Ratovsky et al., 2018; Ratovsky et al., 2020] are manifested at all longitudes, but with different degrees of intensity and latitude coverage.

2. It is noted that there is a dependence of the found correlation coefficient between *TEC* and *AE* on daily variations in *AE* on the first and second days of the storm. The highest correlation and anticorrelation of Δ*TEC* with *AE* are observed for the highest *AE* values.

3. Disturbances of the neutral thermosphere com-

position are demonstrated not to be a key factor in *TEC* disturbances at high latitudes. The high-latitude positive correlation of *TEC* with *AE* can be explained by the behavior of the correlation of T_e with *AE*, which has similar structures at these latitudes at 14–23 UT. An increase (decrease) in *AE* means a rise (fall) in T_e at high latitudes due to strengthening (weakening) of the magnetospheric convection electric field. Note that at high latitudes the positive effects of increasing T_e prevail over the negative effects of increasing n(N2), whereas in the equatorial region the picture is opposite. The highest anticorrelation between Δ*TEC* and *AE* is observed in the equatorial region. This is explained by the behavior of Δn(N2) in the equatorial zone, which correlates well with *AE*.

A similarity in correlations between n(O) and *TEC* disturbances has been found at midlatitudes during daylight hours. It is significant that there is no connection between the correlations of zonal electric field, meridional thermospheric wind, and *TEC* disturbances. According to the correlation analysis results, the relationship between *TEC* and *AE* is explained by the important role of the neutral thermosphere composition disturbances throughout March 17–23, whereas the role of electric field and thermospheric wind disturbances in forming TEC disturbances is crucial only on the first day of the geomagnetic storm.

Space weather data was provided by NASA/GSFC's Space Physics Data Facility's OMNIWeb service [http://omniweb.gsfc.nasa.gov].

The work was financially supported by RSF (Grant No. 21-17-00208) in terms of conducting research using the upper atmosphere model and by the Ministry of Science and Higher Education of the Russian Federation in terms of data analysis.

REFERENCES

Balan N., Alleyne H., Otsuka Y., Vijaya Lekshmi D., Fejer B.G., McCrea I. Relative effects of electric field and neutral wind on positive ionospheric storms. *Earth Planets Space*. 2009, vol. 61, no. 4, pp. 439–445.

Balan N., Otsuka Y., Nishioka M., Liu J.Y., Bailey G.J. Physical mechanisms of the ionospheric storms at equatorial and higher latitudes during the recovery phase of geomagnetic storms. *J. Geophys. Res.: Space Phys*. 2013, vol. 118, iss. 5, pp. 2660–2669. DOI: 10.1002/jgra.50275.

Buonsanto M.J. Ionospheric storms: A review. *Space Sci. Rev*. 1999, vol. 88, pp. 563–601. DOI: 10.1023/A:1005107532631.

Burton R.K., McPherron R.L., Russell C.T. An empirical relationship between interplanetary conditions and *Dst*. *J. Geophys. Res*. 1975, Vol. 80, pp. 4204–4214.

Davis T.N., Sugiura M. Auroral electrojet activity index AE and its universal time variations. *J. Geophys. Res*. 1966. vol. 71, pp. 785–803.

Deminov M.G., Deminova G.F., Depuev V.K., Depueva A.K. Dependence of the F2-layer critical frequency median at midlatitudes on geomagnetic activity. *Solar-Terr. Phys*.. 2017, vol. 3, iss. 4. C. 67–73. DOI: 10.12737/stp-34201707.

Deminov M.G., Deminova G.F., Depuev V.K., Depueva A.Kh. Relation of the Monthly Mean Ionospheric *T* Index to Solar and Geomagnetic Activity Indices. *Geomagnetism and. Aeronomy*. 2021, vol. 61, no. 6, pp. 830–835.

Dmitriev A.V., Suvorova A.V., Klimenko M.V., Klimenko V.V., Ratovsky K.G., Rakhmatulin R.A., Parkhomov V.A. Predictable and unpredictable ionospheric disturbances during St. Patrick's Day magnetic storms of 2013 and 2015 and on 8–9 March 2008. *J. Geophys. Res.: Space Phys*. 2017, vol. 122, iss. 2, pp. 2398–2423, DOI: 10.1002/2016JA023260.

Feshchenko E.Yu., Maltsev Yu.P. Relations of the polar cap voltage to the geophysical activity. *Proc. 26 Annual Seminar. "Physics of Auroral Phenomena"*. Apatity, 2003, pp. 59–61.

Fuller-Rowell T., Codrescu M., Maruyama N., Fredrizzi M., Araujo-Pradere E., Sazykin S., Bust G. Observed and modeled thermosphere and ionosphere response to superstorms. *Radio Sci*. 2007, vol. 42, iss. 4. DOI: 10.1029/2005RS003392.

Gonzalez W.D., Joselyn J.A., Kamide Y., Kroehl H.W., Rostoker G., Tsurutani B.T., Vasyliunas V.M. What is a geomagnetic storm? *J. Geophys. Res.: Space Phys*. 1994, vol. 99, iss. A4, pp. 5771–5792. DOI: 10.1029/93JA02867.

Gonzalez W.D., Tsurutani B.T., Clua de Gonzalez A.L. Interplanetary origin of geomagnetic storms. *Space Sci. Rev*. 1999, vol. 88, pp. 529–562. DOI: 10.1023/A:1005160129098.

Huba J.D., Maute A., Crowley G. SAMI3_ICON: Model of the ionosphere plasmasphere system. *Space Sci Rev*. 2017, vol. 212, pp. 731–742. DOI: 10.1007/s11214-017-0415-z.

Klimenko M.V., Klimenko V.V., Ratovsky K.G., Goncharenko L.P., Sahai Y., Fagundes P.R., de Jesus R., de Abreu A.J., Vesnin A.M. Numerical modeling of ionospheric effects in the middle- and low-latitude F region during geomagnetic storm sequence of 9–14 September 2005. *Radio Sci*. 2011, vol. 46, iss. 3, RS0D03. DOI: 10.1029/2010RS004590.

Klimenko M.V., Klimenko V.V., Zakharenkova I.E., Ratovsky K.G., Korenkova N.A., Yasyukevich Y.V., Mylnikova A.A., Cherniak I.V. Similarity and differences in morphology and mechanisms of the f_0F2 and *TEC* disturbances during the geomagnetic storms on 26–30 September 2011. *Ann. Geophys.* 2017. Vol. 35. P. 923–938. DOI: 10.5194/angeo-35-923-2017.

Klimenko M.V., Klimenko V.V., Despirak I.V., Zakharenkova I.E., Kozelov B.V., Cherniakov S.M., Andreeva E.S., Tereshchenko E.D., Vesnin A.M., Korenkova N.A., Gomonov A.D., Vasiliev E.B., Ratovsky K.G. Disturbances of the thermosphere-ionosphere-plasmasphere system and auroral electrojet at 30° E longitude during the St. Patrick's Day geomagnetic storm on 17–23 March 2015. *J. Atmos. Solar-Terr. Phys*. 2018, vol. 180, pp. 78–92. DOI: 10.1016/j.jastp.2017.12.017.

Lu G., Goncharenko L.P., Richmond A.D., Roble R.G., Aponte N. A dayside ionospheric positive storm phase driven by neutral winds. *J. Geophys. Res*. 2008, vol. 113, iss. A8, A08304. DOI: 10.1029/2007JA012895.

Mayr H.G., Volland H. Magnetic storm characteristics of the thermosphere. *J. Geophys. Res*. 1973, vol. 78, no. 13, pp. 2251–2264.

Mendillo M. Storms in the ionosphere: Patterns and processes for total electron content. *Rev. Geophys*. 2006, vol. 44, iss. 4, RG4001. DOI: 10.1029/2005RG000193.

Mikhalev A.V., Beletsky A.B., Vasilyev R.V., Zherebtsov G.A., Podlesny S.V., Tashchilin M.A., Artamonov M.F. Spectral and photometric characteristics of mid-latitude auroras during the magnetic storm of March 17, 2015. *Solar-Terr. Phys*. 2018, iss. 4, pp. 42–47. DOI: 10.12737/stp-44201806.

Namgaladze A.A., Förster M., Yurik R.Y. Analysis of the positive ionospheric response to a moderate geomagnetic storm using a global numerical model. *Ann. Geophys*. 2000, vol. 18, pp. 461–477. DOI: 10.1007/s00585-000-0461-8.

Pawlowski D.J., Ridley A.J., Kim I., Bernstein D.S. Global model comparison with Millstone Hill during September 2005. *J. Geophys. Res*. 2008, vol. 113, iss. A1. A01312. DOI: 10.1029/2007JA012390.

Pirog O.M., Polekh N.M., Tashchilinet A.V., Romanova

E.B., Zherebtsov G.A. Response of ionosphere to the great geomagnetic storm of September 1998: Observation and modeling. *Adv. Space Res*. 2006, vol. 37, iss. 5, pp. 1081–1087. DOI: 10.1016/j.asr.2006.02.005.

Prölss G.W. Ionospheric F-region storms. *Handbook of Atmospheric Electmdynamics*. CRC Press, 1995, vol. 2, pp. 195–248.

Prölss G.W. Ionospheric Storms at mid-latitude: A short review. *Midlatitude Ionospheric Dynamics and Disturbances*. Washington: American Geophys. Union, 2013. (Geophys. Monograph Ser., 181). DOI: 10.1029/181GM03.

Ratovsky K.G., Klimenko M.V., Klimenko V.V., Chirik N.V., Korenkova N.A., Kotova D.S. After-effects of geomagnetic storms: statistical analysis and theoretical explanation. Solar-Terrestrial Physics. 2018, no. 4, pp. 26–32. DOI: 10.12737/stp-44201804.

Ratovsky K.G., Klimenko M.V., Yasyukevich Y.V., Klimenko V.V., Vesnin A.M. Statistical analysis and interpretation of high-, mid- and low-latitude responses in regional electron content to geomagnetic storms. *Atmosphere*. 2020, vol. 11, iss. 12, 1308. DOI: 10.3390/atmos11121308.

Shpynev B.G., Khabituev D.S., Chernigovskaya M.A. Study of longitudinal irregularities of ionospheric distirbances in the Northern Hemisphere during geomagnetic storms. *Sovremennye problemy distantsionnogo zondirovaniya Zemli iz kosmosa* [Current problems in remote sensing of the Earth from space]. 2018, vol. 15, no. 5, pp. 241–250. DOI: 10.21046/2070-7401-2018-15-5-241-250. (In Russian).

Sojka J.J., Schunk R.W., Denig W.F. Ionospheric response to the sustained high geomagnetic activity during the March'89 great storm. *J. Geophys. Res.* 1994, vol. 99, no. A11, pp. 21341–21352.

Sugiura M. Hourly values of equatorial *Dst* for the IGY. *Annals of the International Geophysical Year*. New York: Elsevier, 1964, vol. 35, pp. 945–948.

Suvorova A.V., Dmitriev A.V., Tsai L.-C., Kunitsyn V.E., Andreeva E.S., Nesterov I.A., Lazutin L.L. *TEC* evidence for near-equatorial energy deposition by 30 keV electrons in the topside ionosphere. *J. Geophys. Res.: Space Phys*. 2013, vol. 118, iss.7, pp. 4672–4695. DOI: 10.1002/jgra.50439.

Vorobjev V.G., Yagodkina O.I. Empirical model of auroral precipitation power during substorms. *J. Atmos Solar-Terr. Phys*. 2008, vol. 70, pp. 654–662.

Yagodkina O.I., Panchenko V.A., Vorobyov V.G., Telegin V.A., Zhbankov G.A. Influence of magnetic activity and solar wind pressure on the mid-latitude ionosphere during a magnetic storm on June 22–23, 2015. *Proc. XLIV Annual Seminar "Phys. of Auroral Phenomena"*. Apatity, 2021, pp. 163–167. DOI: 10.51981/2588-0039.2021.44.038. (In Russian).

Zhang S.-R., Zhang Y., Wang W., Verkhoglyadova O.P. Geospace system responses to the St. Patrick's Day storms in 2013 and 2015. *J. Geophys.Res.: Space Phys*. 2017, vol. 122, iss. 6, pp. 6901–6906. DOI: 10.1002/2017JA024232.

Zolotukhina N.A., Polekh N.M., Mikhalev A.V., Beletsky A.B., Podlesny S.V. Peculiarities of 630.0 and 557.7 nm emissions in the main ionospheric trough: March 17, 2015. *Solar-Terr. Phys*. 2021, vol. 7, iss. 3, pp. 53–67. DOI: 10.12737/stp-73202105.

URL: www.kodak.com/go/imagers (accessed March 30, 2022).

Original Russian version: Belyuchenko K.V., Klimenko M.V., Klimenko V.V., Ratovsky K.G., published in Solnechno-zemnaya fizika. 2022. Vol. 8. Iss. 3. P. 41–48. DOI: 10.12737/szf-83202206.

How to cite this article

Belyuchenko K.V., Klimenko M.V., Klimenko V.V., Ratovsky K.G. Connection of total electron content disturbances with *AE* index of geomagnetic activity during geomagnetic storm in March 2015. *Solar-Terrestrial Physics*. 2022. Vol. 8. Iss. 3. P. 38–45. DOI: 10.12737/stp-83202206.